Electronic Engineering and Informatics
G. Izat Rashed (Ed.)

doi:10.3233/ATDE240060

Multi-Strategy Constant False Alarm Rate Detector in Complex Backgrounds

Cong LIU[a], Pengfei LI[a1], Lu LIU[a], Qi LI[b], Yunqing LIU[b]
[a]*PLA Army Academy of Artillery and Air Defense, Hefei, China*
[b]*Changchun University of Science and Technology, Changchun, China*

Abstract. A multi-strategy switching variability index CFAR (MSVI-CFAR) detector is proposed to further the capability of radar target constant false alarm detection in complex backgrounds. The detector can estimate the clutter background in the reference window. It adaptively selects the optimal detection strategy from the cell-averaging CFAR (CA-CFAR), greatest-of CFAR (GO-CFAR), switching CFAR (S-CFAR), and ordered statistic with cell averaging CFAR (OSCA-CFAR). The results indicate that MSVI-CFAR is beneficial to the detection of SVI-CFAR in the background of uniform background, clutter edge, and multi-target interference and has less CFAR loss and more robust anti-multi-target interference performance.

Keywords. Multi-strategy constant false alarm; Adaptive detection; Target detection

1. Introduction

In modern radars, target detection is usually carried out automatically. Generally, the average power level of clutter is variable and unknown, which requires a constant false alarm detection technology that can adjust the threshold adaptively according to the clutter environment [1]. The traditional mean level (ML) class CFAR and the ordered statistics CFAR (OS-CFAR) [2], as the most classical constant false alarm detectors, are often selected. ML-CFAR mainly includes cell-averaging CFAR (CA-CFAR) [3], greatest-of CFAR (GO-CFAR) [4], and smallest of CFAR (SO-CFAR) [5]. The detection probability of CA-CFAR is optimal in the homogeneous clutter environment, but when the interference is more and the background clutter is more complex, its performance is seriously degraded, and the target is easily obscured. OS-CFAR and SO-CFAR can maintain good performance when dealing with multiple interference targets. However, OS-CFAR will lead to too long data processing time due to the need for sorting, and there is a certain CFAR loss in a uniform environment. SO-CFAR detection performance deteriorates when there is interference in both front and rear sliding windows. GO-CFAR can suppress the false alarm peak in clutter edge background, but it is not good for the performance of multi-target background detection. In the actual environment, the radar background is often very complex, not a uniform background or a specific interference situation, but a non-stationary environment that changes all the time. Simply using a traditional CFAR can no longer meet the needs of target detection in a complex environment but should be targeted at different cluttered background environments.

[1] Corresponding author: Pengfei LI, PLA Army Academy of Artillery and Air Defense, e-mail: congliu@mails.cust.edu.cn

Flexible selection of multiple CFAR strategies is adopted to improve detection probability. Smith and Varshney [6] proposed the variable index CFAR (VI-CFAR) detector, which laid a theoretical foundation for the subsequent multi-strategy CFAR detection. The algorithm is applicable in uniform and clutter edge environments but not in multi-target environments. Li et al. [7] replaced SO-CFAR in the VI-CFAR detector with S-CFAR [8,9] and proposed the switching variability index constant false alarm rate (SVI-CFAR) detector. It improves the performance of VI-CFAR in multi-target environments where interference occurs along both the front and rear sliding windows, but it uses half-window CA-CFAR, which brings additional detection loss.

In this paper, an improved multi-strategy MSVI-CFAR detector is proposed based on the advantages of S-CFAR and OSCA-CFAR [10] for complex clutter environments such as non-uniform and multi-target. The experimental results indicate that MSVI-CFAR maintains the robust performance of VI-CFAR well in uniform environments and clutter edge backgrounds and also performs well in multi-interference targets.

2. MSVI-CFAR Detector Design and Parameter Setting

2.1. SVI-CFAR detector

The SVI-CFAR detector replaces SO-CFAR of VI-CFAR with S-CFAR to solve the problem of multi-target interference. VI is calculated to determine whether the background clutter environment of the front and rear sliding windows is uniform. Then the mean value of the front and rear sliding windows is the same according to the value of MR. Then the CFAR strategy is selected according to the different combinations of VI and MR.

The two statistics, VI and MR, are defined as follows:

$$\mathrm{VI} = 1 + \frac{\hat{\sigma}^2}{\hat{\mu}} = 1 + \frac{1}{N}\sum_{i=1}^{N}\left(y_i - \overline{y}\right)^2 \Big/ \left(\overline{y}\right)^2 = N\sum_{i=1}^{N}\left(y_i\right)^2 \Big/ \left(\sum_{i=1}^{N} y_i\right)^2 \tag{1}$$

$$\mathrm{MR} = \overline{Y}_{\mathrm{A}} \Big/ \overline{Y}_{\mathrm{B}} = \sum_{i\in \mathrm{A}} y_i \Big/ \sum_{i\in B} y_i \tag{2}$$

In the formula, $\overline{y}$ is the arithmetic average of the semi-reference sliding window, $y_i\left(i = 1,2,\cdots,N/2\right)$ is the i sampling value in the reference sliding window, $2N$ is the reference sliding window length, $\hat{\mu}$ and σ^2 are the mean and variance of the sample respectively. $\overline{Y}_{\mathrm{A}}$ and $\overline{Y}_{\mathrm{B}}$ are the sample means of the front and rear sliding windows, respectively. By comparing the VI value and threshold K_{VI}, a judgment is made on whether the front and back sliding windows are in a uniform environment. The hypothesis test formula is as follows:

$$\begin{cases} \mathrm{VI} \le K_{\mathrm{VI}} \Rightarrow \text{Homogeneous environment} \\ \mathrm{VI} > K_{\mathrm{VI}} \Rightarrow \text{Nonhomogeneous environment} \end{cases} \tag{3}$$

By comparing the values of MR with the thresholds K_{MR}^{-1} and K_{MR}, a decision is made on whether the sliding window means are equal. The ruling formula is as follows:

$$\begin{cases} K_{\mathrm{MR}}^{-1} \le \mathrm{MR} \le K_{\mathrm{MR}} \Rightarrow \text{Same mean value} \\ \mathrm{MR} < K_{\mathrm{MR}}^{-1} \text{ or } \mathrm{MR} > \mathrm{K}_{\mathrm{MR}} \Rightarrow \text{Different mean value} \end{cases} \tag{4}$$

The corresponding error probability is:

$$\alpha_0 = P\left[\mathrm{VI} > K_{\mathrm{VI}} \mid \text{Homogeneous environment}\right] \tag{5}$$

$$\beta_0 = 1 - P\left[1/K_{\mathrm{MR}} \le \mathrm{MR} \le K_{\mathrm{MR}} \mid \text{Homogeneous environment}\right] \tag{6}$$

where α_0 is the error probability that the uniform environment is judged to be non-uniform, and β_0 represents that the mean values of the front and rear sliding windows are judged to be different in the uniform environment. According to whether the clutter of the front and rear reference windows is uniform and whether the mean is the same, one of CA-CFAR, GO-CFAR, and S-CFAR is selected adaptively for target detection.

2.2. MSVI-CFAR detector design

Although SVI-CFAR improves the detection performance of VI-CFAR when there is multiple interference in two sliding windows at the same time, SVI-CFAR only uses half-window CA-CFAR for clutter background estimation when there is interference in only one sliding window at the back, which will cause additional CFAR loss. On the other hand, the detection performance of SVI-CFAR decreases in the multi-interference target environment. MSVI-CFAR is proposed on the basis of SVI-CFAR and VI-CFAR. Figure 1 shows the block diagram, and the specific CFAR strategy selection method is shown in Table 1.

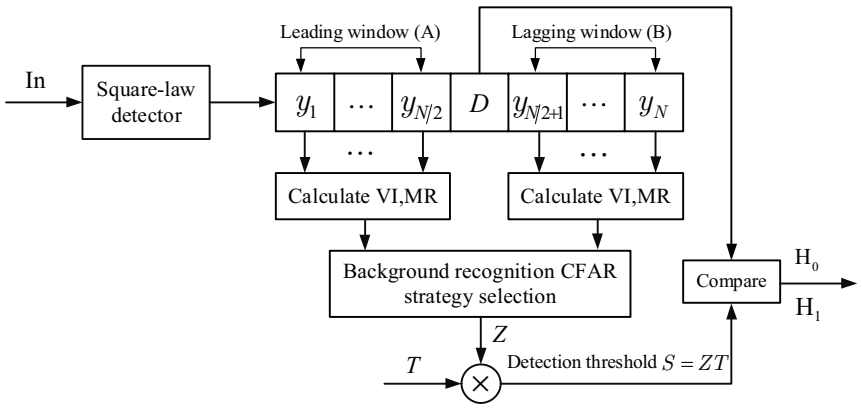

Figure 1. Structure of MSVI-CFAR detector

Table 1. Multiple-strategy selection method of MSVI-CFAR detector

Leading window variable	Lagging window variable	Different means?	MSVI-CFAR Adaptive threshold	Equivalent CFAR method
Yes	Yes	Yes	$C_N \sum_{AB}$	CA-CFAR
Yes	Yes	No	$C_{N/2} \max\left(\sum_A, \sum_B\right)$	GO-CFAR
No	Yes	-	T_s	S-CFAR
Yes	No	-	T_s	S-CFAR
No	No	Yes	$T_{OSCA}\left(y_A(k) + y_B(k)\right)$	OSCA-CFAR
No	No	No	T_s	S-CFAR

2.3. MSVI-CFAR detector parameter selection

The MSVI-CFAR detector adopts the same adaptive selection strategy as the VI-CFAR detector. That is, CA-CFAR, GO-CFAR, S-CFAR, or OSCA-CFAR detection algorithms are selected according to different scenarios. In Table 1, the improved MSVI-CFAR selects different CFAR strategies from adaptation according to statistics VI and MR of the clutter interference environment in the front and rear windows. C_N is the threshold factor of the entire sliding window, $C_{N/2}$ is the threshold factor of the half window, $\sum_{AB}$ is the estimated sum of the entire reference unit sample, $\sum_A$ is the estimated sum of the front sliding window sample, $\sum_B$ is the estimated sum of the back sliding window sample, T_s is the detection threshold of S-CFAR, T_{OSCA}, $y_A(k)$, and $y_B(k)$ are the k -th value of OSCA-CFAR's threshold factor and the order of the front and rear sliding windows, respectively. The specific parameters are set as follows:

In the heterogeneous environment, corresponding to the first row in Table 1, both the front and rear sliding windows are uniform and have the same mean value. In this case, CA-CFAR is selected as the detection method to estimate the entire reference unit to achieve the best detection performance. The parameter values are calculated in Formulas (7) and (8).

$$C_N = \left(P_{fa}\right)^{-1/N} - 1 \tag{7}$$

$$\sum_{AB} = \sum_{i=1}^{N} y_i \tag{8}$$

In the clutter edge scenario, corresponding to the second row in Table 1, the front and rear sliding windows are uniform but have different mean values. Hence, the GO-CFAR strategy can maintain good false alarm control ability. By comparison, GO-CFAR selects the larger value of the sum of samples in the front and back sliding windows as

the estimate of background clutter, that is, $\max\left(\sum_A, \sum_B\right)$. Formulas (9) and (10) show the specific parameter values.

$$C_{N/2} = \left(P_{fa}\right)^{-2/N} - 1 \tag{9}$$

$$\sum_A = \sum_{i=1}^{N/2} y_i \; or \sum_B = \sum_{i=N/2+1}^{N} y_i \tag{10}$$

When there is interference on only one side of the current rear sliding window, that is, corresponding to the third and fourth rows in Table 1, SVI-CFAR chooses half-window CA-CFAR, resulting in certain CFAR loss. MSVI-CFAR replaces half-window CA-CFAR with S-CFAR, which has a similar performance to CA-CFAR under a uniform environment. Moreover, interference can be easily distinguished in multi-target environments, avoiding target masking like CA-CFAR.

In the scenario of multiple jamming targets, the fifth and sixth rows in Table 1 are corresponding. In the sixth row, both the front and rear sliding windows are non-uniform environments, and the mean values are different, indicating that there is a large difference in the amount of interference between the two sliding windows. It will cause one side sliding window to exceed the maximum tolerance of anti-interference ability. Therefore, S-CFAR is chosen to solve the problem of multiple interference targets. In the fifth row, because the mean values of the front and back sliding windows are the same, it indicates that the interference quantity of the two side sliding windows is not much different, and the interference quantity does not exceed the maximum tolerance. OSCA-CFAR is selected to optimize the detection performance. At this time, the detection threshold is $T_{OSCA}\left(y_A(k) + y_B(k)\right)$, where the calculation of the threshold factor is shown in Formula (11) [11]:

$$P_{fa} = \left(\frac{\Gamma(N+1)\Gamma(N-k+1+T_{OSCA})}{\Gamma(N-k+1)\ \Gamma(N+1+T_{OSCA})} \right)^2 \tag{11}$$

3. Simulation Analysis

The MSVI-CFAR is analyzed under uniform background, multi-jamming target background, and clutter edge background through Monte Carlo simulation. The number of Monte Carlo simulations is $M = 10^6$, the length of the reference unit is $N = 24$, $N_t = 12$, false alarm probability $P_{fa} = 10^{-6}$, statistic $K_{\mathrm{VI}} = 4.56$, mean ratio $K_{\mathrm{MR}} = 2.9$. Assuming that the clutter interference background is an exponentially distributed clutter model, the performance of MSVI-CFAR is compared with that of CA-CFAR, GO-CFAR, SO-CFAR, S-CFAR, OSCA-CFAR, VI-CFAR, and SVI-CFAR. The parameter settings of S-CFAR and VI-CFAR are the same as those in [6] and [11], respectively.

3.1. Simulation analysis of detection performance under a homogenous environment

Under a uniform background, Figure 2 shows the comparison of detection performance curves of MSVI-CFAR, where Optimal is the Neyman-Pearson optimal detection curve. CA-CFAR has the best detection performance, and SO-CFAR has the worst one. The detection performance of MSVI-CFAR, SVI-CFAR, and VI-CFAR is close to that of CA-CFAR, and the loss of the above three detectors relative to CA-CFAR is no more than 0.05. In addition, the detection performance of OSCA-CFAR and S-CFAR is between the three and SO-CFAR. OSCA-CFAR has a slightly higher detection performance than S-CFAR.

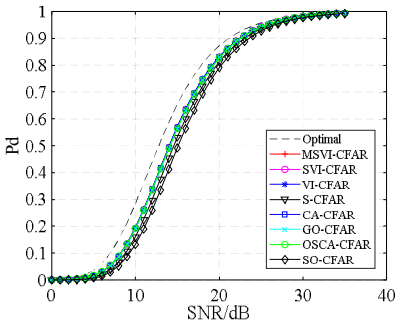

Figure 2. Performance comparison between MSVI-CFAR and other detectors in a homogenous environment

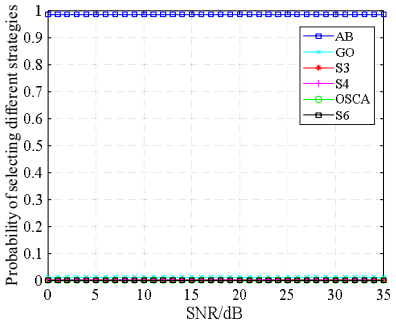

Figure 3. Probability of MSVI-CFAR selecting different strategies in a homogenous environment

Figure 3 shows the probability of MSVI-CFAR selecting different strategies in a homogenous environment, where curve AB represents the power estimation of selecting the entire reference window as the clutter background, corresponding to the first row in Table 1, and the corresponding relationship of other curves is similar. GO is the clutter edge background. At this time, the maximum value estimated by the front and rear sliding windows is selected as the clutter power estimation, corresponding to the second row in Table 1. S3 and S4 show the selection of S-CFAR policies, corresponding to the third and fourth rows in Table 1. OSCA indicates that both the front and rear sliding windows have interference and the mean values are the same, and OSCA-CFAR strategy is selected, corresponding to the fifth row in Table 1. In contrast, S6 indicates that the mean values are different, and S-CFAR is selected to estimate the clutter background, corresponding to the sixth row in Table 1. As can be seen from Figure 3, in the case of uniform clutter background, MSVI-CFAR and VI-CFAR choose the whole reference window as the best strategy for power estimation of clutter background, which is consistent with theoretical analysis.

3.2. Simulation analysis of detection performance of multi-interference targets in clutter background

Figure 4 shows the performance comparison between MSVI-CFAR and other detectors when the front and rear sliding windows each contain three interference targets. As can be seen from the figure, when interference occurs in the current rear slide window, the detection performance of VI-CFAR, CA-CFAR, SO-CFAR, and GO-CFAR decreases sharply. In the scenario of multiple interference targets, VI-CFAR chooses the SO-CFAR

strategy, and the detection performance deteriorates due to the presence of target masking. S-CFAR, MSVI-CFAR, OSCA-CFAR, and SVI-CFAR all maintain good detection performance, among which S-CFAR has the best detection performance, MSVI-CFAR and OSCA-CFAR have similar performance, and both are better than SVI-CFAR. Based on the window selection strategy shown in Figure 5, the reasons why MSVI-CFAR performs better than SVI-CFAR are analyzed. Figure 5(a) shows the window selection strategy probability of MSVI-CFAR. The statistic VI has the same probability of choosing S-CFAR. With the increase of SNR, the probability of choosing OSCA-CFAR and S-CFAR increases, thus improving the detection performance. In Figure 5(b), SVI-CFAR will have a certain CFAR loss when selecting windows A and B, and the detection probability will decrease to a certain extent in the case of multiple interference targets.

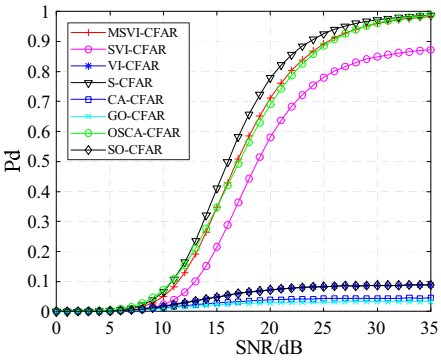

Figure 4. Comparison of the performance of each detector when the front and rear sliding Windows contain three interference targets respectively

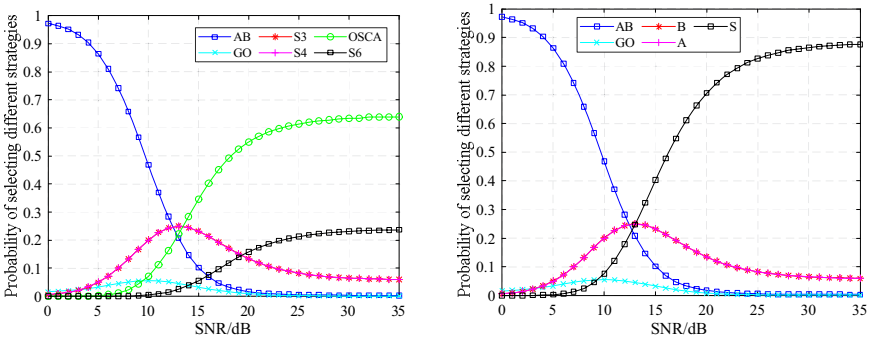

(a) MSVI-CFAR (b) SVI-CFAR

Figure 5. The probability of MSVI-CFAR and SVI-CFAR when the front and rear sliding windows contain three jamming targets respectively

3.3. Simulation performance and analysis in clutter edge environment

Under the clutter edge condition, the SNR is set to 5 dB, and the false alarm probability is $P_{fa} = 10^{-3}$. Figure 6 shows the comparison of the false alarm control ability of the three detectors. It shows that MSVI-CFAR and SVI-CFAR both maintain good false alarm control ability at clutter edge, and their performance is slightly better than that of VI-CFAR.

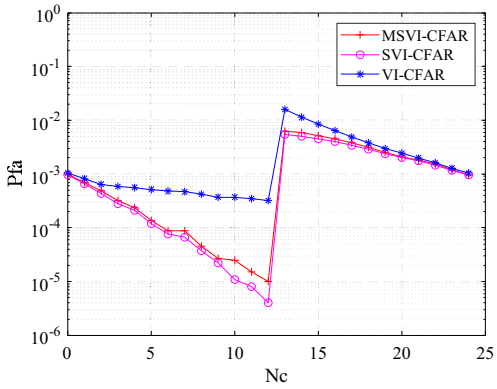

Figure 6. False alarm control ability of each detector in clutter edge environment

4. Conclusions

This article proposes an improved multi-strategy MSVI-CFAR detector based on VI-CFAR and SVI-CFAR to address the issue of poor flexibility and inability to maintain good robustness of conventional radar target CFAR detection techniques in complex clutter environments such as non-uniformity and multiple targets. The detector adopts S-CFAR when the interference occurs in the single-side sliding window, avoiding the constant false alarm loss caused by the half-window CA-CFAR detector. OSCA-CFAR is used to maintain the optimal detection performance when there is interference in both sliding windows, and the mean is the same. The results indicate that the MSVI-CFAR detector maintains a high detection probability in a homogeneous environment. In the multi-target environment, the detection performance is superior to VI-CFAR and SVI-CFAR, and good robustness is maintained. It has good false alarm control ability in a clutter edge environment.

Acknowledgments

Equipment comprehensive research project (LJ20212A011039). This work was supported by the Science and Technology Department Project of Jilin Province (under grant No.20210203039SF).

References

[1] J Cai, S Hu, Y Jin, et al. A CA-CFAR-Like Detector Using the Gerschgorin Circle Theorem for Bistatic Space Based Radar[J]. IEEE Transactions on Aerospace and Electronic Systems, 2021(57-6).

[2] X Liu, D Li. Design and Analysis of Multiple False Targets against Pulse Compression Radar Based on OS-CFAR[J]. IEICE Transactions on Electronics, 2019, 102(6): 495-498.

[3] F D A García, A C F Rodriguez, G Fraidenraich, et al. CA-CFAR detection performance in homogeneous Weibull clutter[J]. IEEE Geoscience and Remote Sensing Letters, 2018, 16(6): 887-891.

[4] H Oudira, A Gouri, A Mezache. Optimization of Distributed CFAR Detection using Grey Wolf Algorithm[J]. Procedia Computer Science, 2019, 158: 74-83.

[5] H Saeedi-Sourck, A Berizi, A Zaimbashi. CFAR Detector in Clutter Edge Situation Using Stationary Wavelet Transform[J]. Advanced Signal Processing, 2017, 2(1): 17-25.
[6] M E Smith, P K Varshney. Intelligent CFAR processor based on data variability[J]. IEEE Transactions on Aerospace and Electronic Systems, 2000, 36(3): 837-847.
[7] Y Li, Z Ji, B Li, et al. Switching variability index based multiple strategy CFAR detector[J]. Journal of Systems Engineering and Electronics, 2014, 25(4): 580-587.
[8] A Salehi, A Zaimbashi, M Valkama. Kernelized-likelihood ratio tests for binary phase-shift keying signal detection[J]. IEEE Transactions on Cognitive Communications and Networking, 2020, 7(2): 541-552.
[9] X W Meng. Comments on 'Constant false-alarm rate algorithm based on test cell information'[J]. Radar Sonar & Navigation Iet, 2009, 3(6): 646-649.
[10] H Chu. Robust Target Detection Methods: Performance Analysis and Experimental Validation[D]. Phoenix: Arizona State University, 2020.
[11] T T V Cao. Constant false-alarm rate algorithm based on test cell information[J]. IET Radar, Sonar & Navigation, 2008, 2(3): 200-213.